https://ntrs.nasa.gov/search.jsp?R=19770026663 2017-08-16T18:33:06+00:00Z

152609

ATS-6 SOLAR CELL EXPERIMENT/IMPROVEMENT

Final Report

NAS Contract No. NAS 5-22873

31 JANUARY 1977

(NASA-CR-152609) ATS-6 SOLAR CELL EXPERIMENT/IMPROVEMENT Final Report, 1 Jan. - 31 Dec. 1976 (Hughes Aircraft Co.) 47 p HC A03/MF A01 CSCL 10A

N77-33607

Unclas

G3/44 50325

Prepared By
LEE GOLDHAMMER
HUGHES AIRCRAFT COMPANY
SPACE AND COMMUNICATIONS GROUP
EL SEGUNDO, CALIFORNIA

Prepared For
GODDARD SPACEFLIGHT CENTER
GREENBELT, MARYLAND 20771

TECHNICAL REPORT STANDARD TITLE PAGE

1. Report No.	2. Government Accession No.	3. Recipient's Catalog No.
4. Title and Subtitle ATS-6 SOLAR CELL EXPERIMENT/ IMPROVEMENT FINAL REPORT		5. Report Date
		6. Performing Organization Code
7. Author(s) L. J. Goldhammer		8. Performing Organization Report No.
9. Performing Organization Name and Address Hughes Aircraft Company Space and Communications Group P.O. Box 92919 Los Angeles, California 90009		10. Work Unit No.
		11. Contract or Grant No. NAS 5-22873
12. Sponsoring Agency Name and Address Goddard Space Flight Center Greenbelt, Maryland		13. Type of Report and Period Covered Final Report, 1 January 1976 to 31 December 1976
		14. Sponsoring Agency Code
15. Supplementary Notes		

16. Abstract

The ATS-6 solar cell flight experiment (SCFE) includes a small solar panel holding 16 different solar cell configurations and two identical signal processing units. The panel is mounted to the external surface of the environment measurements experiment (EME), which is a package of eight scientific experiments, including the SCFE. The EME package is located on a structure atop the base of the 30 foot parabolic reflector of the ATS-6 spacecraft. The ATS-6 spacecraft was successfully launched into synchronous orbit on 30 May 1974. On 2 June 1974, the first meaningful data were received from the solar cell experiment.

ATS-6 SCFE data through 2 years of synchronous orbit operation are presented. Comparisons are made of the performances of the 13 different types of solar cell/cover configurations, including new cover processes and materials, and the COMSAT violet cell. These performances are also compared 1) to the performances of the LES-6 solar cell experiment, the ATS-6 main solar arrays, and the Hughes Aircraft Company solar arrays, and 2) to laboratory spectrum electron irradiations. It was found that the cells of the ATS-6 experiment generally performed as expected through 6 to 9 months in orbit, but that at 2 years they were more severely degraded than expected.

17. Key Words (Selected by Author(s))	18. Distribution Statement
Flight experiment Solar cells Temperature coefficients Electron irradiation	

19. Security Classif. (of this report)	20. Security Classif. (of this page)	21. No. of Pages	22. Price*
Unclassified	Unclassified	45	

*For sale by the Clearinghouse for Federal Scientific and Technical Information, Springfield, Virginia 22151.

TECHNICAL CONTENT STATEMENT

This final report for The ATS-6 Solar Cell Flight Experiment (SCFE) Extension/Improvement Project summarizes the results of the flight data through 2 years of synchronous oribt operation and is submitted for approval to the National Aeronautics and Space Administration, Goddard Space Flight Center. This report contains information prepared by Hughes Aircraft Company under NASA Contract 5-22873. Its contents are not necessarily endorsed by the National Aeronautics and Space Administration.

ACKNOWLEDGEMENT

The author is grateful to J. S. Powe, who spent many long hours upgrading the data analysis computer program and running the data through the computer.

PRECEDING PAGE BLANK NOT FILMED.

CONTENTS

		Page
1.	SUMMARY	1
2.	INTRODUCTION	3
3.	FLIGHT HARDWARE DESCRIPTION	5
	Solar Cell Configuration	5
	Solar Panel	6
	Signal Processing Unit	7
	Calibration of Solar Cells	9
	Software Upgrade	9
	Temperature Coefficient Results	10
4.	IN-ORBIT OPERATION	17
5.	IN-ORBIT RESULTS	19
6.	CONCLUSIONS	35
7.	NEW TECHNOLOGY	37
8.	REFERENCES	39

PRECEDING PAGE BLANK NOT FILMED

ILLUSTRATIONS

		Page
1	ATS-6 SCFE Solar Panel	2
2	ATS-6 EME Package	2
3	ATS-6 Spacecraft	4
4	Front View of the ATS-6 SCFE Solar Panel	5
5	Solar Cell/Relay Configuration	8
6	SPU Current Section	8
7	SPU Voltage Section	8
8	Normalized I_{sc} at 40° Angle as a Function of Coverglass Thickness	10
9	Solar Cell Temperature Profile Characteristics as a Function of 1MeV Electron Fluence	11
10	Rigid Solar Panel Temperature for the ATS-6 Solar Cell Experiment	17
11	In-Orbit Normalized Cell Parameters	22
12	Uncorrected Current-Voltage Characteristics for Cells of Configuration 13	33
13	Maximum Power Performance of Six Configurations Through 2 Years in Orbit	34

PRECEDING PAGE BLANK NOT FILMED

TABLES

		Page
1	ATS-6 Solar Cell Flight Experiment Configurations	6
2	Classical "Temperature Coefficients" for the ATS-6 Correlation Solar Cells	15
3	Photovoltaic Comparisons at 25°C and AMO Intensity	20
4	Percentage I_{sc} Degradation after 50 Days in Orbit, Ultraviolet Effects	21
5	Solar Cell Degradation after 2 Years in Orbit	23

EDING PAGE BLANK NOT FILMED

1. SUMMARY

ATS-6 solar cell flight experiment data through 2 years of synchronous orbit operation are presented. Comparisons are made of the performances of the 13 different types of solar cell/cover configurations, including new cover processes and materials, and the COMSAT violet cell. These performances are also compared 1) to the performances of the LES-6 solar cell experiment, the ATS-6 main solar arrays, and the Hughes Aircraft Company solar arrays, and 2) to laboratory spectrum electron irradiations. It was found that the cells of the ATS-6 experiment generally performed as expected through 6 to 9 months in orbit, but that at 2 years they were more severely degraded than expected.

Included in this report are the results of the temperature coefficient test conducted with the correlation cells.

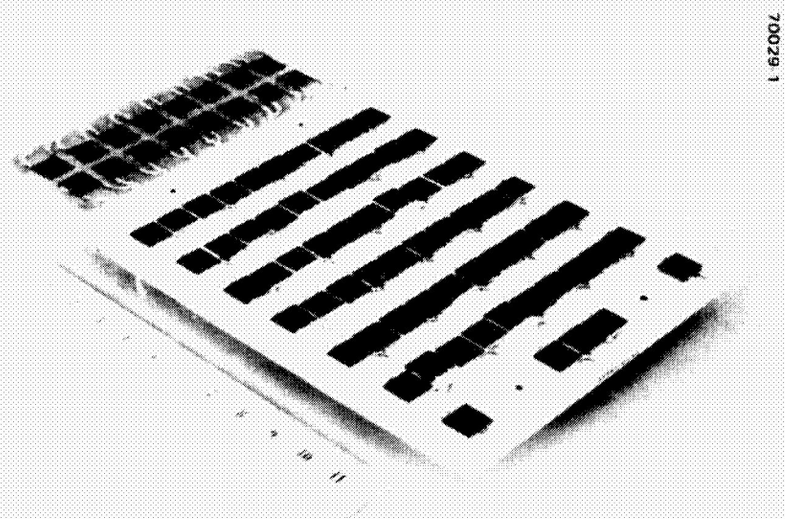

FIGURE 1. ATS-6 SCFE SOLAR PANEL (PHOTO 4R 32030)

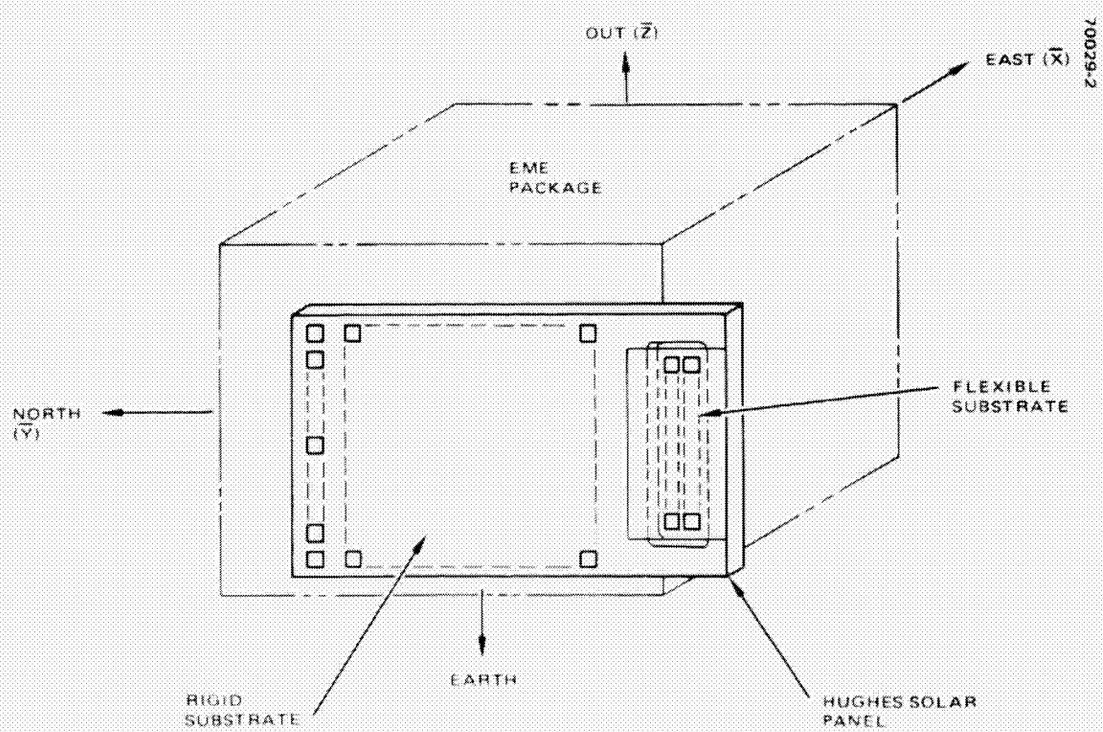

FIGURE 2. ATS-6 EME PACKAGE

REPRODUCIBILITY OF THE
ORIGINAL PAGE IS P

2. INTRODUCTION

The solar cell flight experiment (SCFE) consists of a small solar panel and two identical signal processing units. The panel (Figure 1) contains 65 solar cells on the rigid substrate and 16 solar cells (one cell being inactive) on the flexible substrate. The panel is mounted to the external surface of the environmental measurements experiment (EME), which is a package of eight scientific experiments including the SCFE (Figure 2). The EME package is located on a structure atop the base of the 9.1 meter parabolic reflector of the ATS-6 spacecraft (Figure 3). The SCFE package incorporates 80 individual 2 x 2 cm solar cells, with real time telemetry providing 12 V-I data points for each individual solar cell and five temperature data points for sampling solar cell temperature.* The experiment requires 24 seconds for complete data sampling and transmission and is operated at programmed intervals throughout the ATS-6 mission life. Data are retrieved from the SCFE for approximately 3 minutes, resulting in each cell being sampled six to eight times each time the experiment is turned on.

The three-axis stabilized ATS-6 spacecraft was successfully launched into synchronous orbit on 30 May 1974. Injection occurred at 19:30:49 GMT into a near-perfect orbit. On 2 June 1974 at 0:10:14 GMT, the first meaningful data were received from the solar cell experiment. Since then, data were received from the experiment once a day for the first 3 months and once a week thereafter. The solar cell experiment is activated when the sun is normal to the axis vertical to the west face of the spacecraft. The EME package is rotated 13° about the spacecraft Z-axis in order to align the package with the normal direction of the magnetic field lines at final east longitude. Therefore, when the solar panel is activated, sun angles from +38° to -12° are encountered.

The primary ATS-6 SCFE objectives are to isolate and identify the solar cell degradation mechanism(s) resulting from particulate radiation and to obtain specific design data applicable to extended synchronous spacecraft missions. Specific objectives of this experiment are:

1) Compare ground base simulator cell measurements with the in-space current voltage characteristics

*Because of combined failures of SPU2 and the thermistors, solar cell open circuit voltages were used to determine in-flight operating temperatures (see Section 4).

2) Study cover glass assembly transmittance losses caused by ultraviolet (UV) and particulate radiation

3) Correlate space radiation effects as a function of cover glass thickness

4) Study the effect of both base resistivity (2 and 10 ohm-cm) and cell thickness (0.020 and 0.030 cm) on cell performance in a synchronous environment

5) Compare the performance of COMSAT's violet cell to conventional cells

6) Study the effects of radiation of the back surface of cells with minimal shielding

7) Study the effect of space environment on the solar cell for advanced shielding materials: fluorinated ethylene propylene (FEP) and 7940 and 7070 integral covers

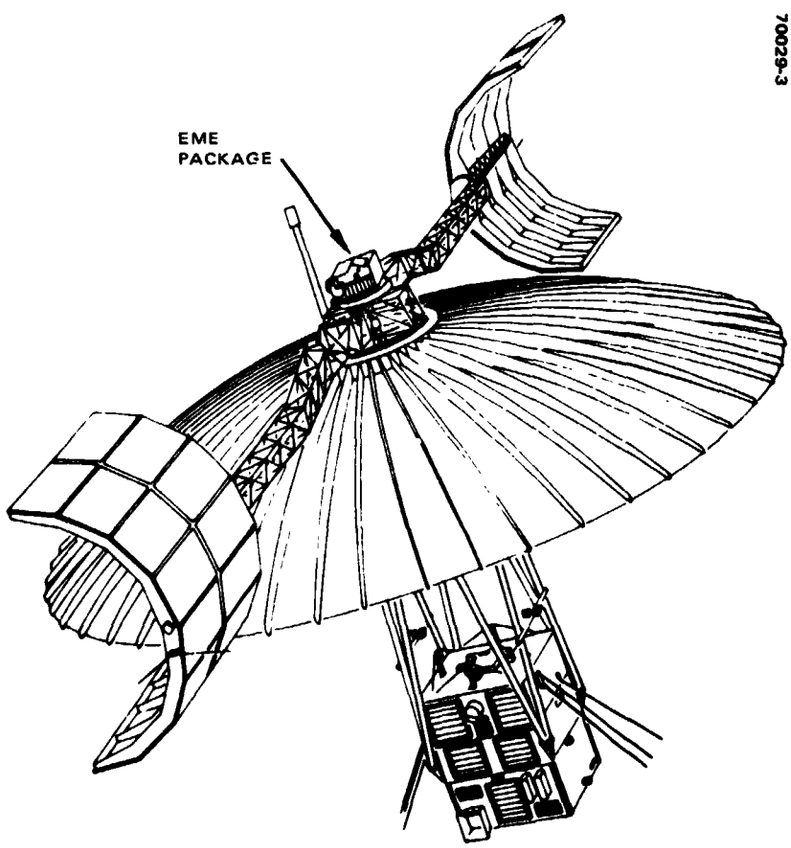

FIGURE 3. ATS-6 SPACECRAFT

3. FLIGHT HARDWARE DESCRIPTION

SOLAR CELL CONFIGURATION

A major objective established for the ATS-6 SCFE was to fly those cell types that would provide the most meaningful data to spacecraft designers. The solar cell sample selection for the flight panel is summarized in Table 1. All cells chosen for the flight experiment are 2 x 2 cm in size; all of the flight cells were manufactured by Heliotek (Spectrolab); except for a five-cell sample of violet cells made by COMSAT Laboratories. A single lot of Dow Sylgard 182 adhesive was used to bond the solar cell covers, except as indicated in Table 1. Similarly, all cover glasses were formed from Corning 7940 fused silica and had 0.41 μm UV cutoff filters, except as shown. Solar cells for configurations 6 and 7 were supplied to ION Physics to have integral covers applied. Solar cells for configurations 10 and 13 were supplied to NASA Lewis Research Center for FEP application.

Each of the 16 configurations listed in Table 1 contains five identical cell assemblies. Figure 4 is the front view of the SCFE and shows the individual solar cell locations. (See also Table 3.) Configurations 1 through

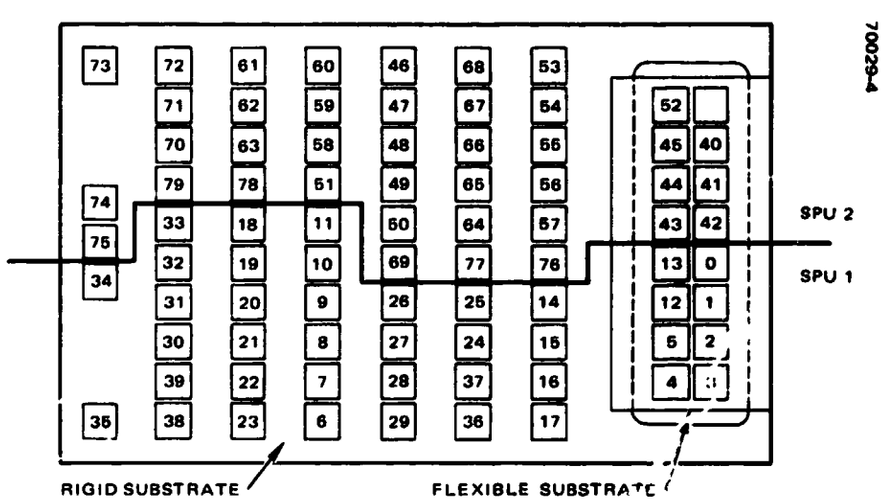

FIGURE 4. FRONT VIEW OF THE ATS-6 SCFE SOLAR PANEL

TABLE 1. ATS-6 SOLAR CELL FLIGHT EXPERIMENT CONFIGURATIONS

Configuration	Resistivity, ohm-cm	Cell Thickness, cm	Cover Glass Thickness, cm	Remarks	Location
1	10	0.030	0.0076		Rigid
2	10	0.030	0.015		Rigid
3	10	0.030	0.030		Rigid
4	10	0.030	0.076		Rigid
5	10	0.030	0.0076	Plain 7940 fused silica cover; no filter or coatings on cover	Rigid
6	10	0.030	0.0038	7940 integral cover	Rigid
7	10	0.030	0.0076	7070 integral cover	Rigid
8	2	0.030	0.015		Rigid
9	2	0.020	0.015		Rigid
10	10	0.030	0.015	Cover without UV filter; cover adhesive of 0.005 cm FEP	Rigid
11	10	0.020	0.015		Rigid
12	1	0.025	0.015	COMSAT violet cell; cerium doped microsheet cover without UV filter	Rigid
13	10	0.030	0.013	FEP cover without added adhesive	Rigid
14	10	0.020	0.015		Flexible
15	2	0.020	0.015		Flexible
16	2	0.030	0.015		Flexible

13 are installed on the rigid portion of the panel; configurations 14 through 16 are installed on the flexible portion. In the majority of cases, the selected cells are boron-doped n/p, 10 ohm-cm resistivity, 0.030 cm thick, and have solder-coated silver-titanium (AgTi) contacts. The fused silica covers are bonded to the cells to very tight tolerances. This eliminates the presence of any gaps between the contact bars and cover glass edges, thus precluding low energy proton damage because of an exposed cell active area. Ohmic contacts are coated with RADAC, a radiation coating, to prevent low energy proton damage through areas of thin solder coverage.

SOLAR PANEL

The SCFE solar panel, 25 x 43 cm, contains 80 active solar cells. The solar panel is mounted on the west face of the EME package so that the backside of the rigid portion of the solar panel faces the EME package and

the flexible portion extends beyond the EME package as shown in Figure 2. The protruding flexible panel allows radiation to impinge on the rear of the cells mounted on the flexible panel.

The rigid substrate is a 0.64 cm (0.25 inch) thick aluminum honeycomb with 0.025 cm (0.010 inch) thick aluminum face sheets. An insulating paint is applied to the aluminum face sheet to insulate the solar cells from the aluminum. The solar cells are individually mounted to the substrate using an RTV silicone rubber adhesive. The cells on the rigid substrate are framed within aluminized teflon, a mirror-like material that aids in reducing the panel temperature.

A 6.9 x 21 cm hole was cut in the rigid substrate to allow for attachment of the flexible substrate section. The flexible substrate is a composite laminate of 0.025 mm thick fiberglass cloth and 0.025 mm thick Kapton. This 0.050 mm composite laminate is stretched across the hole and bonded to a 0.15 cm thick fiberglass doubler. Each cell of this section is symmetrically mounted over holes cut out in the doubler so that approximately 80 percent of the cell back surface is covered with only the 0.05 mm flexible substrate material. All cell types on the flexible panel are duplicated on the rigid panel to obtain comparative data on the radiation effect on the back surface of the cell; however, for reasons to be defined later, this comparative data is presently unavailable.

A group of 20 cells is individually wired to one of four panel connectors, each of which is connected to one of two signal processing units (SPUs). Separate lead wires are provided for voltage and current sensing. The ground return from each cell is connected to a common ground.

SIGNAL PROCESSING UNIT

The SPU is located inside the EME package interfaces between the solar panels and the ATS encoder. Each SPU measures the I-V characteristics of 40 solar cells using 12 precisely known loads and provides temperature information. The experiment carries two SPUs so that the total of 80 cells may be analyzed. In operation, one of the 40 solar cells is connected to one of the 12 load resistors by relays (Figure 5). Thus, only two relays are energized within each SPU at any one time. In order to measure cell characteristics, one cell select relay is energized while the unit is sequenced through the load select relays. Each load is connected for 30 ms. During that time, each SPU output is sampled and telemetered once. The encoder then outputs a pulse that is used to increment the load relays. The process is repeated for each of the 40 solar cells.

Cell current is determined from the voltage developed across an accurately known load resistor (Figure 6). Cell voltage is measured differentially across a cell (Figure 7). The voltage measurement lines are separate from the cell current lines so that line drops are eliminated from the readings. Both SPUs derive their power from a single experimenter payload regulator. The SCFE experiment is turned on and off by a ground

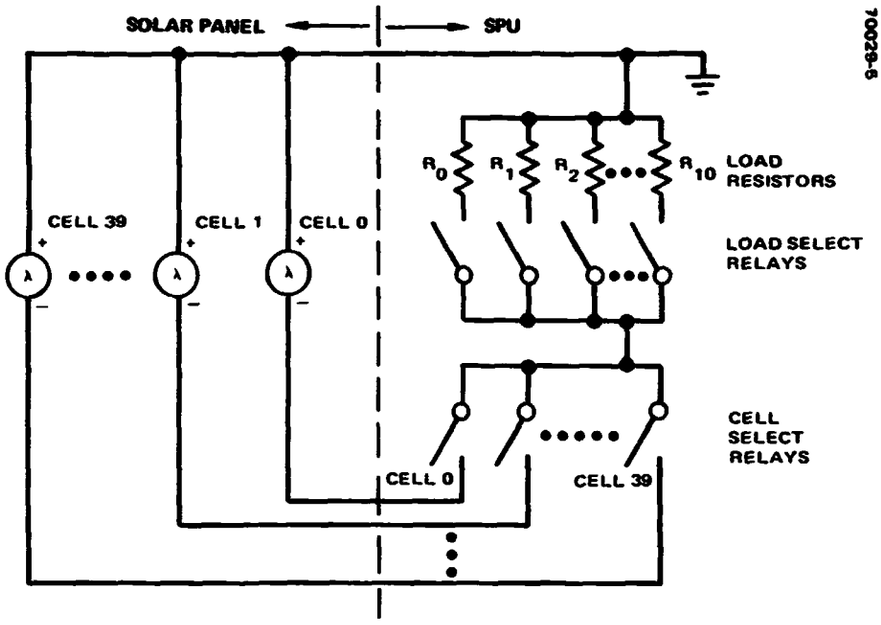

FIGURE 5. SOLAR CELL/RELAY CONFIGURATION

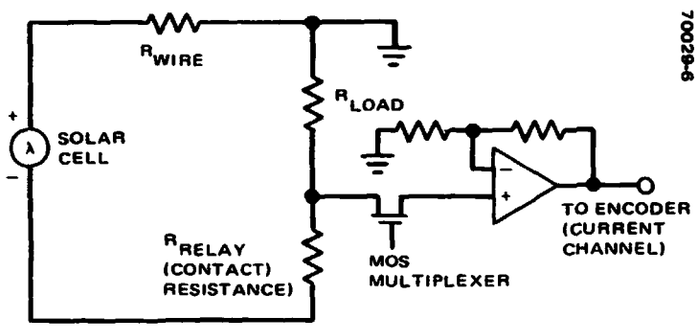

FIGURE 6. SPU CURRENT SECTION

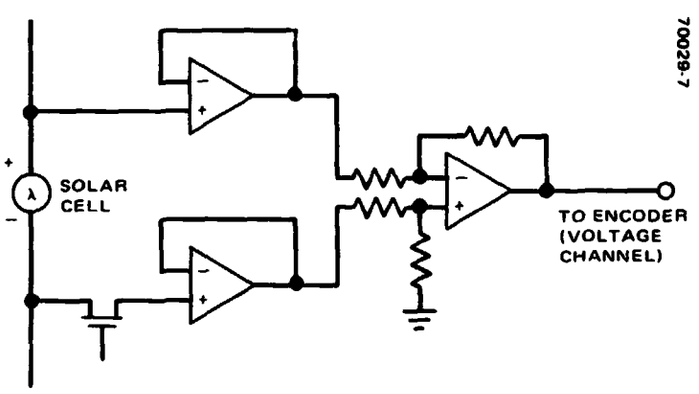

FIGURE 7. SPU VOLTAGE SECTION

command that controls the payload regulator. A more complete description of the experiment operation may be found in the Final Report of Contract NAS 5-11677 (Reference 1).

CALIBRATION OF SOLAR CELLS

Electrical measurements using the Spectrolab X25L solar simulator were made on each solar cell before and after applying a cover glass. Solar cell assemblies for each configuration were placed into three groups (for qualification panel, flight panel, and correlation samples) such that each group represented the total configuration population. The COMSAT violet cells were first electrically measured using COMSAT's X25L solar simulator. The cells sent to Hughes Aircraft Company were chosen by COMSAT and were closely matched to each other. After the installation of the cells in the solar panel and after each qualification test of the solar panel, the solar cells were electrically measured on the Hughes pulsed xenon solar simulator (Reference 2). A secondary balloon flight standard (Hughes A1A) at a setting of 0.0712 volt was used as the cell standard for the flight panel under pulsed xenon testing.

SOFTWARE UPGRADE

Early results of the flight experiment (References 3, 4) indicated that the short circuit currents of the cells in space were higher by 1 to 8 percent than measurements made with ground-based solar simulators. The curve factor in space was also observed to be much softer at the higher in-orbit temperature than predicted. These phenomena resulted in conducting two ground tests — an angle of incidence test and temperature coefficient test — on the ATS-6 correlation cells. As mentioned above, these cells are from the original solar cell and coverglass purchase for the flight configuration and represent, as closely as possible, the cells in orbit.

The sun angle of the experiment varies from +38° to -12°. The cosine function was previously employed (References 3, 4) to correct the cell's current to sun normal intensity and give reasonably accurate results for angles less than 25°. An angle of incidence test on the correlation cells was performed to determine the corrections to the cells' parameters at the higher sun angles (Reference 5). The results of this test were input to the computer software. Figure 8 summarizes the test results for the normalized I_{sc} as a function of cover glass thickness at a 40° angle. The normalized value of I_{sc} is compared to the value of the cosine of 40°. An improvement in the cell performance (over that obtained using the cosine function) as a function of increased cover glass thickness is observed. As shown in Figure 8, the output of the cells covered with 0.076 cm (30 mil) covers (configuration #4) is approximately 4 percent higher than that obtained using the cosine function; thus, an error to current of 4 percent is introduced into the results of the data reduction when using the cosine function. Figure 8 also shows that the cells with no antireflecting coatings (configurations 6 and 7) have lower I_{sc} values than the cosine function would predict.

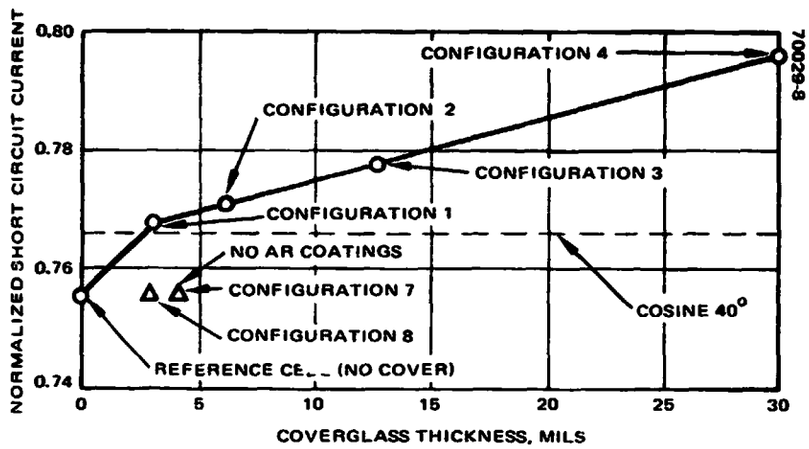

FIGURE 8. NORMALIZED I_{sc} AT 40° ANGLE AS A FUNCTION OF COVER GLASS THICKNESS

TEMPERATURE COEFFICIENT RESULTS

A "temperature coefficient" test was performed on 58 correlation cells to determine the temperature profile of the cells at the higher in-space temperatures. This test also included the effect of electron irradiation on the temperature profiles of these cells. Figure 9 displays the results of the temperature profile as a function of electron fluence level. Figure 9a shows the temperature profile as a function of electron fluence level for the 10 ohm-cm, 0.030 cm (12 mil) thick solar cells. This figure represents the temperature profile for configurations 1 through 7, 10, and 13. As the figure shows, the voltage parameters are linear as a function of radiation level. The current parameters are for the most part nonlinear, except the preirradiation value of I_{sc}. At 100°C the current curve factor (Imp/Isc) is 0.854, which is considerably different than the value used in the old ATS-6 computer program. This is probably the main reason why the in-space current and power values at 25°C were greater than the ground based values as reported in References 3 and 4.

Figure 9b displays the temperature profile for the 10 ohm-cm, 0.020 cm (8 mil) thick solar cells. Figure 9b represents the temperature profile for configurations 11 and 14. The slope for I_{sc} as a function of temperature appears to be greater than for the 0.030 cm thick cells; 21.5 versus 16.8 $\mu A/cm^2 °C$. I_{mp} does not behave as nicely as for the 0.030 cm thick cells, but this may be mainly due to the small sample size (2 to 3 cells) contributing to the uncertainty.

Figure 9c shows the temperature profiles for the 2 ohm-cm, 0.030 cm (12 mil) thick solar cells (configurations 8 and 16). The temperature profile of I_{sc} for the 2 ohm-cm cell appears to increase more rapidly than for the 10 ohm-cm. Also, the temperature profile for I_{sc} appears to remain linear as a function of radiation level. The temperature profile of I_{mp} for the 2 ohm-cm cells is reasonably flat over the temperature range tested. This

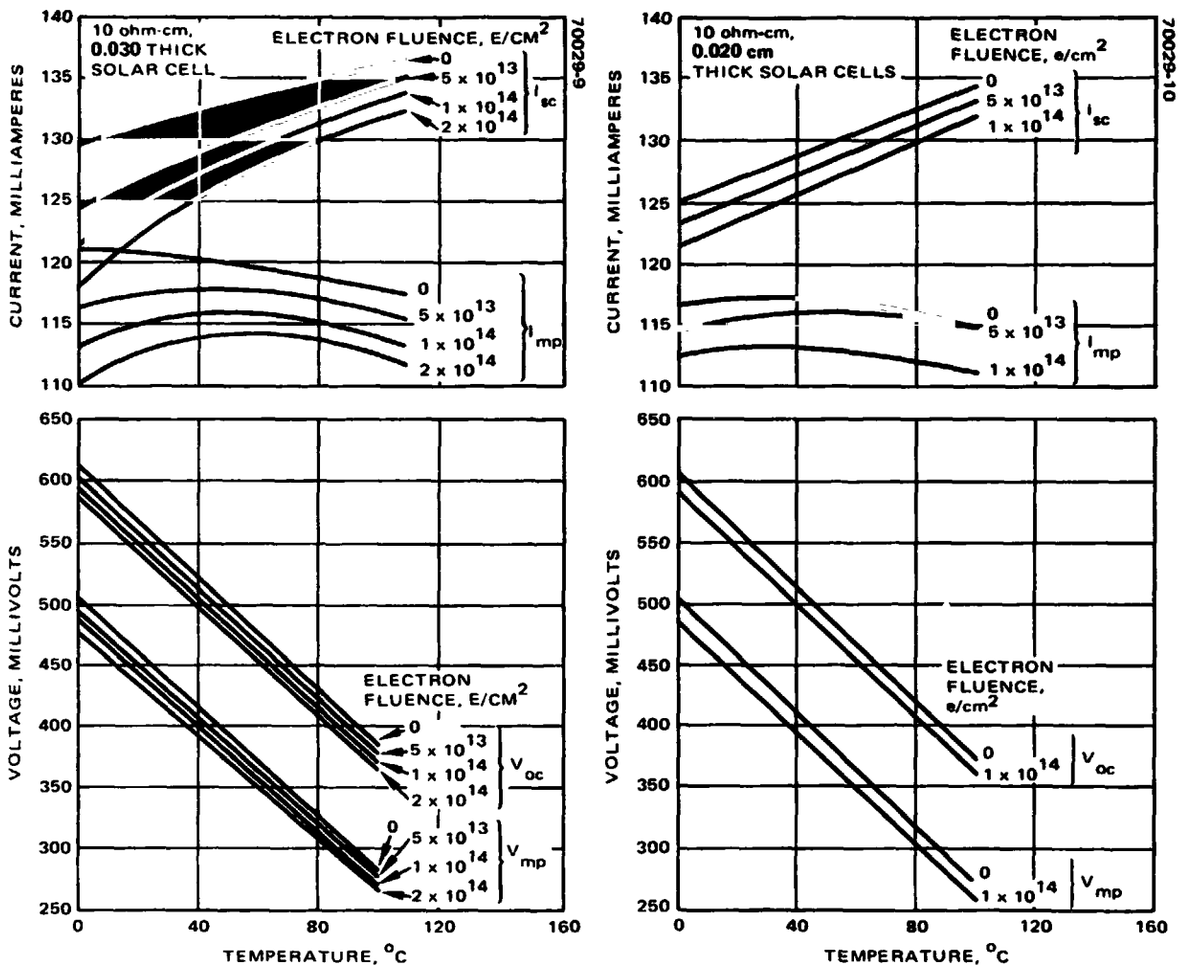

a) CONFIGURATIONS 1 THROUGH 7, 10 and 13

b) CONFIGURATIONS 11 AND 14

FIGURE 9. SOLAR CELL TEMPERATURE PROFILE CHARACTERISTICS AS A FUNCTION OF 1 MeV ELECTRON FLUENCE

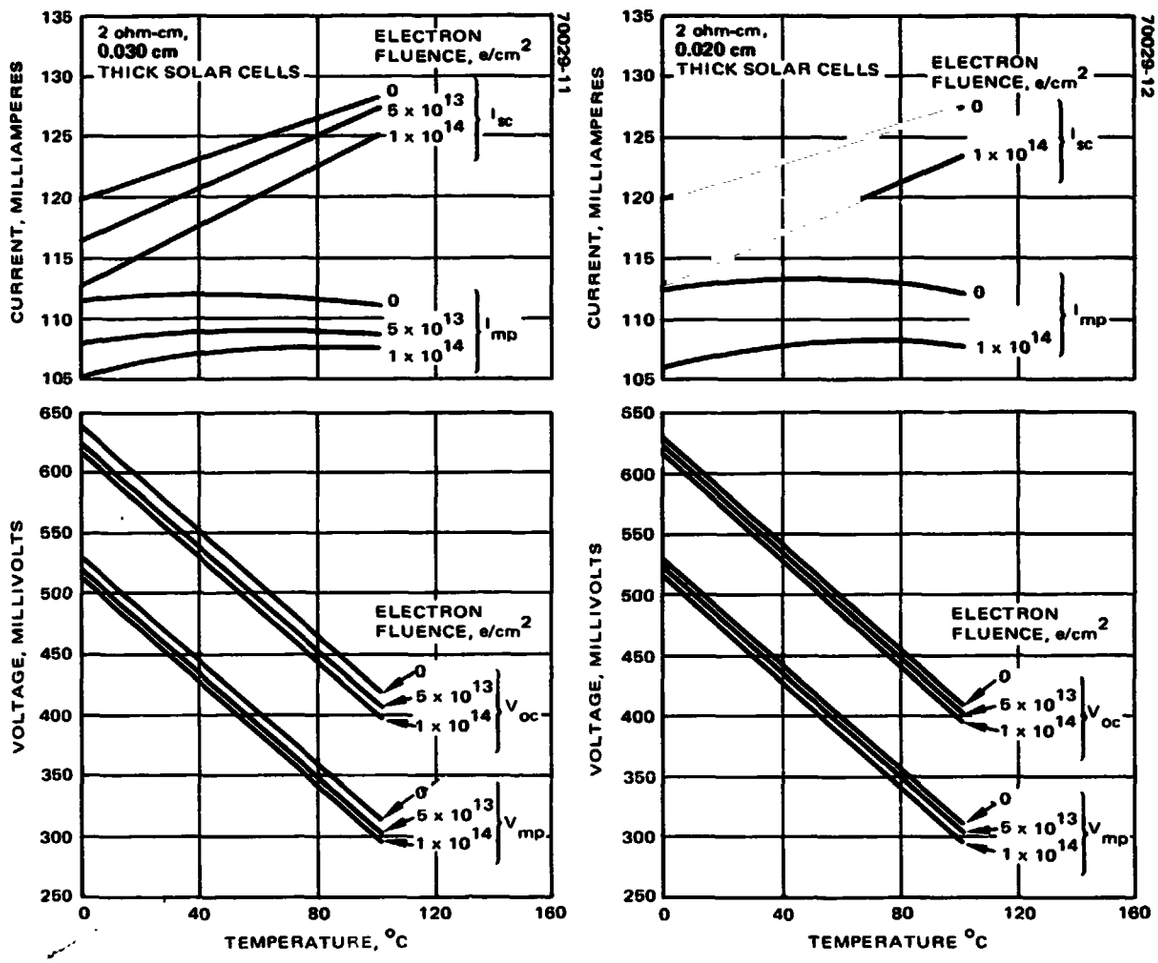

c) CONFIGURATIONS 8 AND 16

d) CONFIGURATIONS 9 AND 15

FIGURE 9 (CONTINUED). SOLAR CELL TEMPERATURE PROFILE CHARACTERISTICS AS A FUNCTION OF 1 MeV ELECTRON FLUENCE

is quite different than the 10 ohm-cm cells where the slope of I_{mp} is negative as a function of increasing temperature. The voltage temperature profile is not as steep for the 2 ohm-cm as for the 10 ohm-cm solar cells. This results in slightly less voltage loss at higher temperatures for the 2 ohm-cm than for the 10 ohm-cm solar cells.

Figure 9d shows the temperature profile for the 2 ohm-cm, 0.020 cm thick solar cells (configurations 9 and 15). The temperature profiles for the 2 ohm-cm, 0.020 cm thick cells are quite similar to the 2 ohm-cm, 0.030 cm thick cells; the absolute current values of the thicker cells are higher.

Figure 9e displays the temperature profile for the violet solar cells of COMSAT Laboratories. This solar cell is a 1 ohm-cm, 0.025 cm (10 mil) high efficiency solar cell (configuration 12). The current temperature profile is the steepest of all the cell types tested. The current capability of the cell at 25°C and at 100°C is the highest of all cells tested. As a function of radiation level, the slope of current became even steeper, going from 25° $\mu A/cm^2 {}^\circ C$ at preirradiation to 49.3 $\mu A/cm^2 {}^\circ C$ at 1×10^{14} e/cm^2. Another interesting feature of this cell's current temperature profile is that I_{mp} has a positive slope for increasing temperature after being irradiated. No other cell type tested demonstrated this phenomenon. Although the absolute voltage capability of the violet cells was higher than the 2 ohm-cm cells, the temperature profile (slope) was about the same.

In an attempt to condense the results, the classical temperature coefficients were calculated and are displayed in Table 2 for each configuration and radiation level. Temperature coefficients are defined as the slope of the cell parameters as a function of temperature. The voltage temperature coefficient represents the entire temperature range because the profiles are very nearly linear over the temperatures tested. The current temperature profiles, for the most part, are nonlinear functions of temperature. Therefore, the current temperature coefficients are only estimates of the slope between 25° and 100°C. The author feels that these current coefficients should only be used to indicate trends and not to be used as prediction tools. For prediction purposes, the actual change to the cell parameters (Figure 9) as a function of the temperature should be used.

Reference 6 documents the test procedure and the detailed results of the temperature coefficient tests. The software program was upgraded using the results of this test. The temperature profiles for I_{sc}, I_{mp}, V_{mp}, and V_{oc} for each configuration were implemented as a function of fluence level. A two-dimensional interpolation technique was employed to determine the change of the cell parameters due to temperature as a function of electron fluence level.

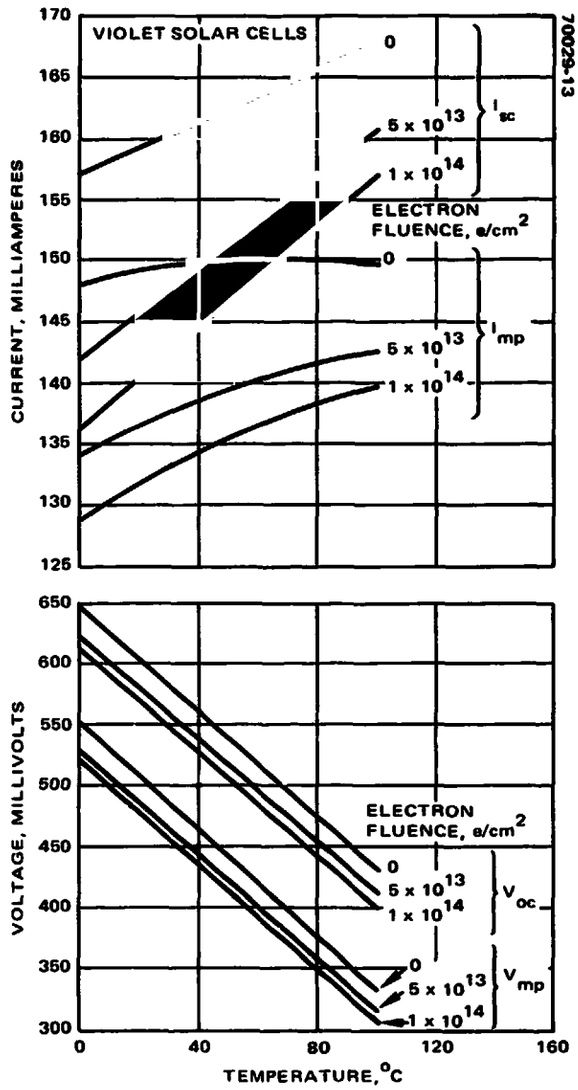

e) CONFIGURATION 12

FIGURE 9 (CONTINUED). SOLAR CELL TEMPERATURE PROFILE CHARACTERISTICS AS A FUNCTION OF MeV ELECTRON FLUENCE

TABLE 2. CLASSICAL "TEMPERATURE COEFFICIENTS" FOR THE ATS-6 CORRELATION SOLAR CELLS

Configuration	Sample Size	Electron Fluence, e/cm^2	Solar Cell Coefficients*			
			Open Circuit Voltage, $mV/^oC$	Voltage at Maximum Power, $mV/^oC$	Short Circuit Current*, $\mu A/cm^2{}^oC$	Current at Maximum Power*, $\mu A/cm^2{}^oC$
Reference cell	20	0	-2.24	-2.14	16.8	-15.7
	5	5×10^{13}	-2.26	-2.13	26.9	- 2.4
	5	1×10^{14}	-2.22	-2.09	27.2	- 3.6
	5	2×10^{14}	-2.22	-2.12	30.0	- 3.8
2	4	0	-2.24	-2.16	19.1	-11.2
	4	2×10^{14}	-2.21	-2.14	34.0	- 1.4
3	5	0	-2.25	-2.20	15.8	-13.2
	5	1×10^{14}	-2.25	-2.18	27.1	- 7.0
6	5	0	-2.25	-2.21	13.7	-16.6
	2	5×10^{13}	-2.22	-2.10	20.9	-19.0
	3	1×10^{14}	-2.19	-2.11	27.2	- 0.9
7	5	0	-2.27	-2.22	15.5	-14.2
	2	5×10^{13}	-2.27	-2.21	22.0	- 1.0
	3	1×10^{14}	-2.25	-2.15	26.5	- 5.5
8	4	0	-2.17	-2.14	19.2	- 2.7
	1	5×10^{13}	-2.12	-2.18	27.3	0.0
	3	1×10^{14}	-2.16	-2.14	29.6	+ 3.7
9	5	0	-2.12	-2.11	19.7	- 2.3
	2	5×10^{13}	-2.20	-2.20	20.3	- 3.2
	3	1×10^{14}	-2.19	-2.18	22.5	- 2.2
11	5	0	-2.37	-2.31	21.5	-11.5
	2	5×10^{13}	-2.20	-2.11	25.8	-13.6
	3	1×10^{14}	-2.30	-2.23	24.7	- 9.3
12	5	0	-2.15	-2.18	25.0	- 0.9
	2	5×10^{13}	-2.09	-2.12	43.1	+14.3
	3	1×10^{14}	-2.10	-2.11	49.3	+22.4

*Slope between 25° and 100^oC.

4. IN-ORBIT OPERATION

When data are acquired from the experiment, the temperature of the rigid solar panel ranges between 56° and 91°C (Figure 10). (The flexible panel appears to be running warmer.) The solar panel sun angle is obtained from data furnished by the solar aspect sensor of the EME package and varies between +38° and -12°C. The sun angle uncertainty is 1°, a value that results in a negligible error at sun-normal conditions and 1.3 percent error at the high sun angles. Some of the scatter observed in the data can be attributed to the uncertainty in the sun angle.

The current channel of SPU 2 failed some time before the flight experiment was activated, causing loss of data from half of the solar cells and from three thermistors. Since the solar cells from each configuration were divided between each SPU, only statistics were affected — the sample size of each configuration was reduced from five cells to two or three cells. One thermistor connected to SPU 1 also failed, leaving only one thermistor on the flexible panel determining temperature. Upon reviewing the data from this thermistor on the flexible panel, it has been determined that the readings are erroneous and cannot be used. To correct this deficiency, the open circuit voltage of four cells on configurations 3 and 4 is being used to determine the temperature of the cells on the rigid panel.

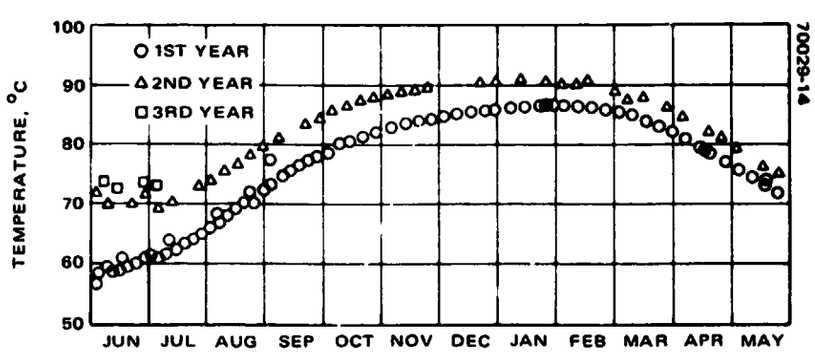

FIGURE 10. RIGID SOLAR PANEL TEMPERATURE FOR THE ATS-6 SOLAR CELL EXPERIMENT

PRECEDING PAGE BLANK NOT FILMED

5. IN-ORBIT RESULTS

All data through 2 years of operations, including the previously published results (References 3, 4), were run through the upgraded version of the Hughes solar array prediction program (Reference 7). The results of all photovoltaic characteristics presented herein are reduced to standard conditions of normal incidence, 25°C and AMO intensity. Table 3 shows the average solar cell characteristics for the first 5 days, 50 days, and 765 days in orbit compared to the prelaunch pulsed xenon solar simulator cell values. The beginning of life comparison indicates that the short circuit current of all configurations on the rigid panel is higher (5 to 10 mA) for the space data than for the current under the solar simulators. The offset in the current in space is not a function of any cell type; therefore, the higher current observed for the cells in space is most likely an electronic offset of the SPUs and not higher performance of the cells. The open circuit voltages of the cells on the rigid panel were on the average reasonably close to the ground based measurements, -10 to +4 mV. This difference is well within the ability to determine the solar panel temperature. The maximum power was greater (up to 6 percent) for the in-space data, which, in turn, reflects the current offsets and voltage uncertainty.

The V_{OC} of the cells in configurations 14, 15, and 16 indicates that the flexible panel is running considerably warmer than the rigid panel. With the thermistor behaving anomalously, the exact temperature of the cells on the flexible panel is very difficult to determine. One difficulty in calculating the temperature is that the EME package temperature louvers are immediately behind the flexible panel. Exactly what quantities of heat are released by these louvers is dependent on the requirements of the EME package. With additional information, the temperature of the flexible panel might possibly be determined and the data from the cells reduced. In this report, however, only the data from the cells of the rigid panel will be reported.

Comparing the photovoltaic characteristics of the cells on the rigid panel for the first 5 days in orbit shows that the violet cells have the highest output of all configurations, about 26 percent higher than the conventional 2 ohm-cm cells. The cells with covers but without antireflection coating (configurations 5, 6, and 7) are down in I_{SC} about 3 to 9 percent (with 0.0038 cm (1-1/2 mil) 7940 integral cover the lowest) compared to configurations 1 and 2. The 2 ohm-cm cells exhibit a greater maximum power capability over the 10 ohm-cm cells for both cell thicknesses. The open

PRECEDING PAGE BLANK NOT FILMED

TAB'.E 3. PHOTOVOLTAIC COMPARISONS AT 25°C AND AMO INTENSITY
(Ground Measurements Versus Space Data)

						Space Data											
		Pulsed Xenon Simulator				2 to 7 Days in Orbit				50 Days in Orbit				765 Days in Orbit			
Configu ration	Cell	I_{sc} mA	V_{oc} mV	P_{mp} mW	Curve Factor	I_{sc} mA	V_{oc} mV	P_{mp} mW	Curve Factor	I_{sc} mA	V_{oc} mV	P_{mp} mW	Curve Factor	I_{sc} mA	V_{oc} mV	P_{mp} mW	Curve Factor
1	10	140	558	56 3	0 724	149	554	59 1	0 718	145	552	57 3	0 714	127	542	49 2	0 715
	15	140	553	57 7	0 744	149	550	60 2	0 734	148	549	59 7	0 733	130	543	51 9	0 738
	22	138	553	57 2	0 752	147	556	60 6	0 744	144	556	59 4	0 740	122	544	49 6	0 743
2	25	141	560	57 9	0 734	149	550	59 1	0 721	148	549	58 0	0 716	130	542	50 2	0 716
	38	139	554	57 4	0 744	149	554	60 2	0 731	146	552	58 6	0 728	122	540	48 2	0 728
3	8	138	550	56 7	0 745	144	544	57 5	0 733	141	543	56 0	0 729	125	537	48 9	0 731
	16	140	550	57 5	0 746	146	548	59 0	0 738	146	548	58 6	0 734	129	543	51 2	0 732
4	19	141	559	58 0	0 723	146	552	58 0	0 719	143	551	56 6	0 719	124	544	48 0	0 712
	35	139	549	56 7	0 744	144	559	59 5	0 742	142	557	58 0	0 735	122	549	49 4	0 734
	37	141	551	57 4	0 740	146	549	58 4	0 729	144	549	57 6	0 729	127	545	50 4	0 728
5	28	139	562	58 7	0 751	144	557	59 2	0 741	139	554	56 7	0 737	119	545	48 0	0 740
	30	139	561	58 8	0 755	145	564	60 5	0 739	141	560	57 3	0 727	120	549	47 8	0 726
6	6	127	553	52 6	0 747	136	548	54 3	0 727	136	545	52 8	0 715	120	534	45 6	0 713
	24	127	549	51 8	0 744	136	541	53 7	0 733	135	539	53 1	0 727	120	532	46 5	0 729
	31	128	559	53 4	0 749	138	554	55 8	0 730	136	551	54 1	0 723	117	540	46 1	0 729
7	9	131	550	53 3	0 763	141	544	56 4	0 736	138	542	54 7	0 732	120	536	47 5	0 737
	14	131	557	54 8	0 754	138	540	54 5	0 731	138	539	54 2	0 729	122	534	48 1	0 735
8	11	131	589	59 0	0 764	140	576	60 1	0 743	136	575	57 4	0 735	117	560	48 6	0 742
	23	132	592	60 2	0 771	140	589	62 1	0 754	137	589	60 6	0 751	117	573	50 8	0 759
	27	131	591	59 8	0 773	138	584	60 9	0 757	136	583	59 6	0 753	117	570	50 7	0 760
9	20	126	575	56 7	0 782	135	569	58 6	0 762	133	568	57 2	0 759	114	558	48 0	0 756
	36	126	578	56 6	0 778	135	564	58 0	0 759	134	564	57 0	0 754	116	555	48 6	0 754
10	21	142	561	56 6	0 711	146	556	58 8	0 724	143	556	57 8	0 725	120	546	48 5	0 736
	29	142	561	59 9	0 .53	147	554	60 3	0 739	145	553	588	0 734	124	544	49 6	0 739
	39	140	551	56 5	0 735	146	547	58 8	0 728	143	545	56 7	0 728				
11	7	131	549	54 1	0 751	140	542	56 1	0 741	137	541	54 8	0 740				
	17	133	547	54 2	0 746	141	536	55 6	0 736	141	536	55 3	0 734	124	532	48 5	0 736
	32	134	542	54 7	0 753	140	544	56 9	0 749	137	542	55 4	0 747	118	535	47 4	0 752
12	26	166	601	78 0	0 784	176	598	81 8	0 776	173	595	79 5	0 772	143	574	62 9	0 767
	33	167	598	78 0	0 779	179	598	83 1	0 776	174	594	80 0	0 773	141	573	61 8	0 764
13	18	146	558	59 8	0 735	151	553	60 1	0 720	149	549	58 4	0 714	125	470	35 0	0 595
	34	144	558	60 4	0 749	150	560	62 6	0 747	147	558	61 1	0 743	120	468	33 9	0 606
14	0	133	548	53 6	0 735	144	483	48 2	0 695	142	486	47 8	0 694	125	495	43 3	0 702
	3	134	548	53 3	0 726	146	494	49 8	0 689	144	496	49 3	0 689	128	503	44 6	0 696
	12	130	541	53 7	0 760	142	488	48 6	0 703	140	491	48 5	0 705	125	498	44 2	0 709
15	1	126	576	54 9	0 753	139	512	49 9	0 701	137	515	49 4	0 699	121	518	43 6	0 699
	4	125	575	54 9	0 768	135	522	51 4	0 729	134	524	50 9	0 727	117	524	44 6	0 729
	13	125	580	55 4	0 765	137	516	50 8	0 718	136	518	50 2	0 715	120	521	44 6	0 716
16	2	130	586	58 1	0 763	140	524	52 7	0 715	138	526	51 8	0 710	119	525	45 0	0 722
	5	131	594	59 0	0 755	142	536	53 8	0 706	140	538	53 0	0 703	122	535	46 5	0 714

REPRODUCIBILITY OF THE ORIGINAL PAGE IS POOR

circuit voltages of all cells followed the trends as predicted by their base resistivities and cell fabrication processes.

Table 3 displays the cell characteristics in space after 50 days in orbit (~400 sun hours considering cosine effects). Results from irradiation ground test performed at Hughes Aircraft Company (Reference 8) indicate that damage from UV rays is nearly saturated after 400 to 500 sun hours. Only minimum damage to the cells from the particulate environment is expected in this short period; therefore, losses to I_{sc} should indicate damage from UV effects. As summarized in Table 4, the configurations with the standard UV filters bonded with adhesive degraded in I_{sc} by 1.6 ±0.7 percent.

Configuration 5, covers with no UV filter bonded with adhesive, degraded slightly more, 3.3 ±0.1 percent. Results from UV ground tests (Reference 8) indicated degradation to adhesive without UV filter protection would be much greater than observed on configuration 5. Another very interesting result is that FEP used as either an adhesive or a cover degraded to a degree almost identical to that of the standard adhesive/UV filter configuration, 1.8 ±0.1 percent. The I_{sc} of the violet cells degraded slightly more than the cells with the standard covers and UV filter (2.3 ±0.9 percent), but this difference is not statistically significant. The data indicate that degradation to I_{sc} due to UV effects (excluding integral covers) is about 2 percent for all configurations except unfiltered bonded coverglass, which is approximately 3 percent. The effect to integral covered cells is about 1 percent.

Figure 11 displays the normalized cell degradations through 2 years in orbit for each cell. Profiles for configurations 1 through 13 are shown. Each point in Figure 11 is an average of 5 days of data. The absolute cell performance of each cell is available from the author upon request. The performance of I_{sc}, I_{mp}, V_{mp}, V_{oc}, and P_{max} are plotted through 2 years of operation. The degradation profiles of configurations 1 to 4 are those of the 10 ohm-cm, 0.030 cm thick cells where coverglass thickness was varied (0.0076 to 0.076 cm thick). As appears, the degradation profile of V_{oc} is well-behaved, but I_{sc} and P_{mp} of some cells for a given configuration diverge in their rates of degradation. Each cell's degradation profile is

TABLE 4. PERCENTAGE I_{sc} DEGRADATION AFTER 50 DAYS IN ORBIT, ULTRAVIOLET EFFECTS

Identification	Average Percentage I_{sc} Loss
Standard UV filter (configurations 1, 2, 3, 4, 8, 9, and 11)	1.6 ± 0.7
Integral covers (configurations 6 and 7)	0.8 ± 1.1
FEP adhesive and covers (configurations 10 and 13)	1.8 ± 0.1
Violet cell (configuration 12)	2.3 ± 0.9
No UV filter (configuration 5)	3.3 ± 0.1

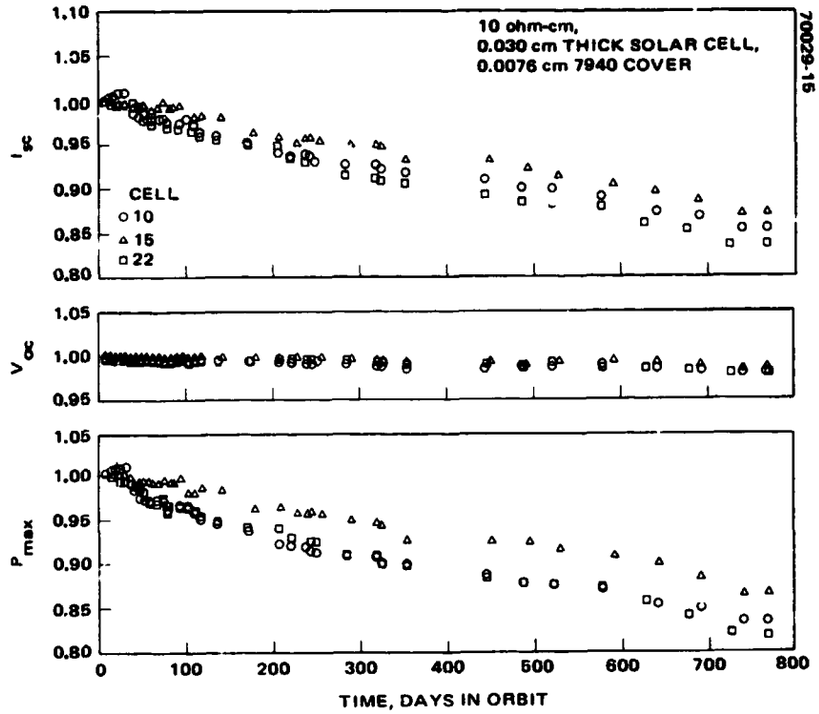

a) CONFIGURATION 1

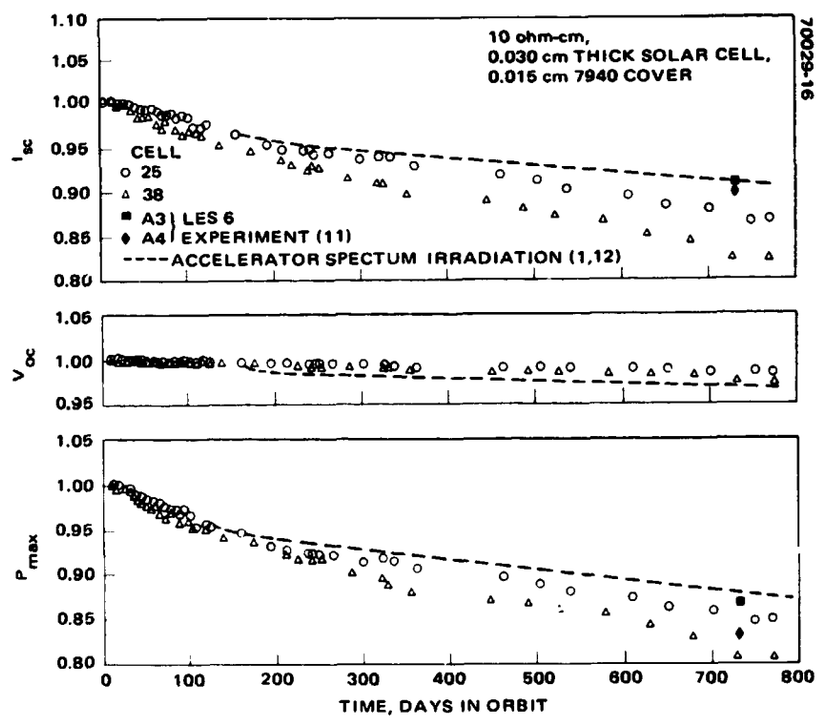

b) CONFIGURATION 2

FIGURE 11. IN-ORBIT NORMALIZED CELL PARAMETERS

consistent within itself. Table 5 shows the average percentage loss for each configuration. As is indicated, there is a slight trend in the average percentage degradation as a function of cover thickness. The exact degradation profile of ATS-6 experiment cells as a function of cover thickness cannot be deduced because differences in degradation profiles of the individual cells overshadow the effect of cover thickness variation.

Displayed with the profiles of configurations 2 and 3 are the results of laboratory spectrum electron irradiations on the ATS-F ground test cells (References 1, 9) with covers of the same thickness. The electron spectrum was an attempt to produce a fluence-energy spectrum closely approximating the model spectrum for synchronous altitude (Reference 10). The cells were mounted on a cylindrical aluminum drum which was rotated during the irradiation, effectively producing a fluence field of cylindrical symmetry. To compare with the degradation in space, 2 percent additional degradation was added to the laboratory results to account for UV effects. The V_{oc} degradations in space of the cells with 0.015 and 0.030 cm thick covers agree within 1 percent of the laboratory irradiations. However, the I_{sc} and P_{mp} degradations did not agree well at all with the laboratory results. Degradations were more severe at 2 years in space. The spectrum irradiation profiles for I_{sc} and P_{mp} followed the space degradation for approximately 150 and 300 days in orbit for 0.015 and 0.030 cm thick covers, respectively.

The cells of configuration 2 are quite similar to cells A3 and A4 of the LES-6 SCFE (Reference 11). The 2-year degradations of cells A3 and A4 are indicated in the profile for configuration 2. The I_{sc} degradations are

TABLE 5. SOLAR CELL DEGRADATION AFTER 2 YEARS IN ORBIT

Configuration	Average Percentage Loss		
	I_{sc}	V_{oc}	P_{mp}
1	14.7 ± 2.0	1.8 ± 0.5	16.3 ± 2.6
2	15.3 ± 3.9	2.0 ± 0.9	17.4 ± 4.3
3	12.7 ± 1.7	1.1 ± 0.4	14.1 ± 1.6
4	14.2 ± 1.3	1.3 ± 0.6	15.3 ± 2.2
5	17.2 ± 0.4	2.4 ± 0.5	20.0 ± 1.9
6	13.0 ± 2.2	2.2 ± 0.5	15.6 ± 2.3
7	12.8 ± 2.8	1.4 ± 0.4	13.7 ± 3.5
8	16.1 ± 1.0	2.6 ± 0.8	18.0 ± 1.4
9	15.0 ± 1.5	1.9 ± 0.3	17.1 ± 1.7
10	16.8 ± 1.3	1.8 ± 0.3	17.6 ± 0.2
11	14.0 ± 3.2	1.1 ± 0.7	14.7 ± 3.5
12	19.4 ± 2.0	4.2 ± 0.1	24.4 ± 2.2
13	18.6 ± 2.4	15.7 ± 1.4	43.2 ± 3.5

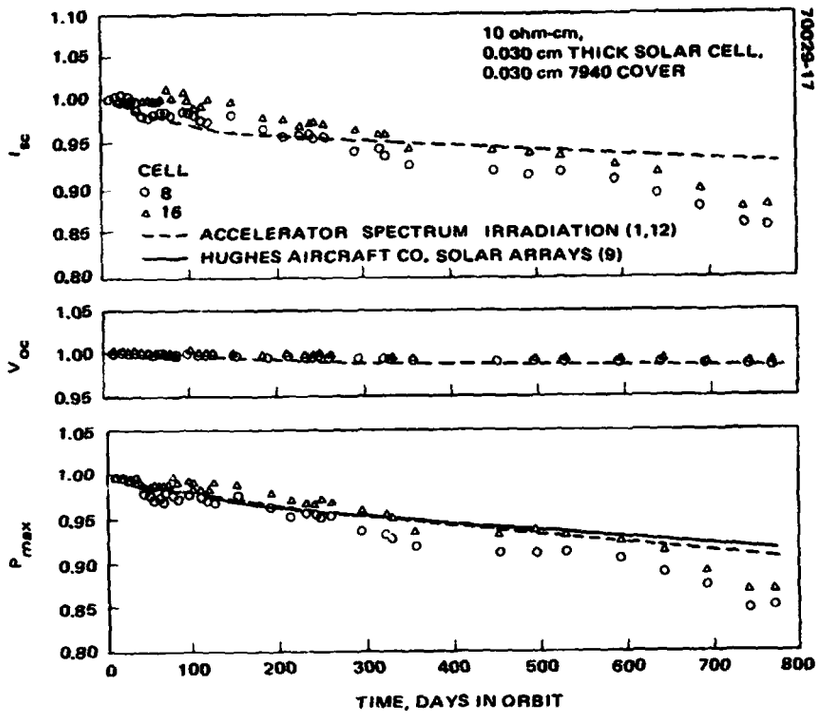

c) CONFIGURATION 3

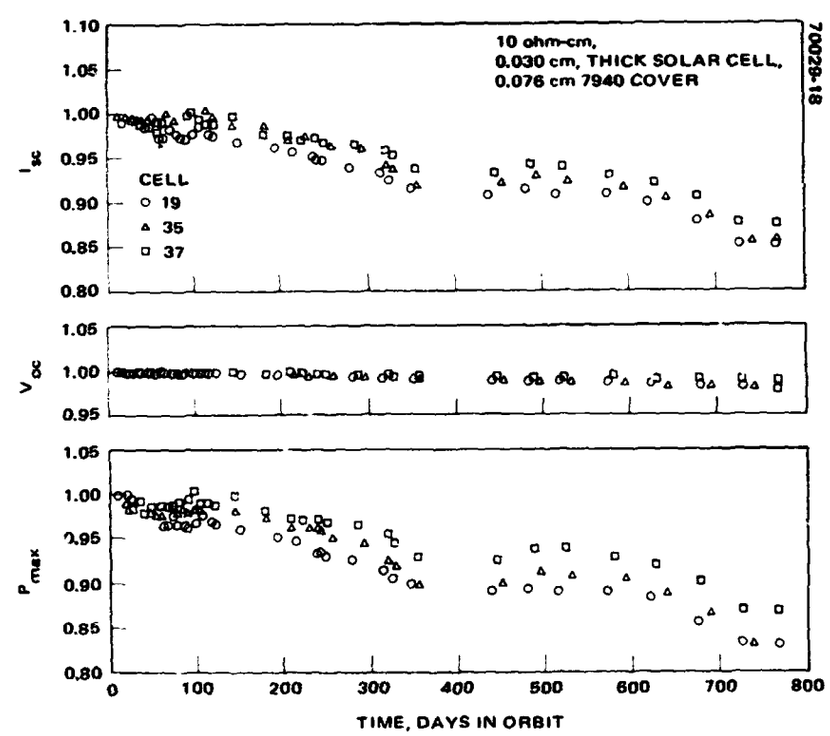

d) CONFIGURATION 4

FIGURE 11 (CONTINUED). IN-ORBIT NORMALIZED CELL PARAMETERS

less than those of the ATS-6 cells but very close to the spectrum irradiation results. The P_{mp} degradations are both more severe than the spectrum irradiation results and very close to the degradation of the ATS-6 cells. Cell A4 of the LES-6 has no MgF antireflection (AR) coating on the cover; however, the I_{sc} currents of this cell and cell A3 track within 1 percent, so the MgF coating cannot make the difference. It is interesting to note that the two cells of LES-6 also display the same differences in degradation profile for both I_{sc} and P_{mp} as seen with ATS-6.

Also displayed for configuration 3 is the maximum power degradation profile as indicated from Hughes Aircraft Company solar arrays in synchronous orbit. The flight performance of the TACSAT, Intelsat IV, Intelsat IVA, Anik, and WESTAR solar arrays was determined for orbital durations over 5 years (Reference 12). Again, the cells of the ATS-6 experiment display more degradation at 2 years in orbit than has been observed on other Hughes solar arrays. It appears that degradations of ATS-6 experiment cells agree only through approximately 300 days in orbit.

The I_{sc} and P_{mp} cell parameters of configuration 4 display a cyclic degradation profile, considerably more pronounced than in configurations 1, 2, and 3. Configuration 4 has the 0.076 cm thick cover glass. The effect shown in the figure could be due to additional angle of incidence effects caused by an unpredictable contribution of intensities from the surface of the panel, which is aluminized teflon.

The configuration 5 profile displays the normalized cell parameters for the cells protected with a 0.0076 cm (3 mil) thick 7940 coverglass with no UV filter or AR coating. Cells of configuration 1 are these cells' counterpart, having a 0.0076 cm thick cover with UV filter and AR coating. The degradation profiles of configuration 5 cells behave very much alike. They do not exhibit the same dispersion in the data as has been seen in the profiles for configurations 1 to 4. However, as in the case of configuration 4, the cyclic nature of the profile is pronounced. As shown in the configuration 5 profile, I_{sc} degrades more rapidly during the first 100 days in orbit than it does in configuration 1. This is due to the UV degradation to the unprotected adhesive. This same degradation profile is indicated in P_{max}. After 2 years in orbit, the average I_{sc} degradations of configurations 1 and 5 are 14.7 and 17.2 percent, respectively. This difference of approximately 3 percent is most likely due to additional degradation of the adhesive. It would be interesting to see whether degradation of the unprotected adhesive continues.

Profiles for configurations 6 and 7, the integral covered cells, show normalized cell parameters. Again, there is considerable dispersion in the individual cell degradation profiles. The averaged degradation after 2 years in orbit (Table 5) of I_{sc} for configurations 6 and 7 are 13.0 and 12.8 percent, respectively. This is approximately 2 percent less than the degradation of configuration 1, cells with the bonded 0.0076 cm thick 7940 coverglass. The difference is most likely owing to the additional degradation to the cover adhesive. No low energy proton type damage was observed on either integral

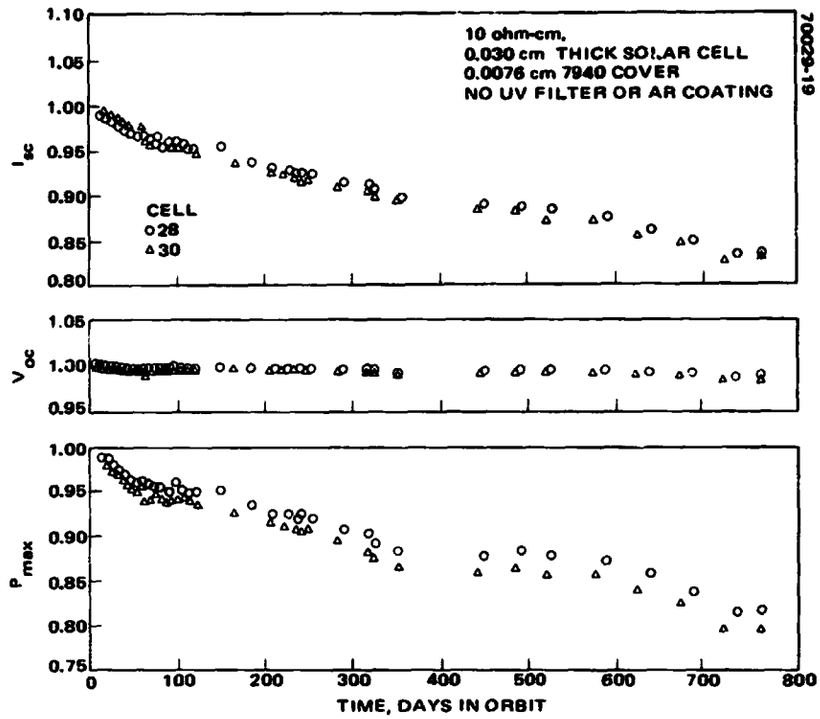

e) CONFIGURATION 5

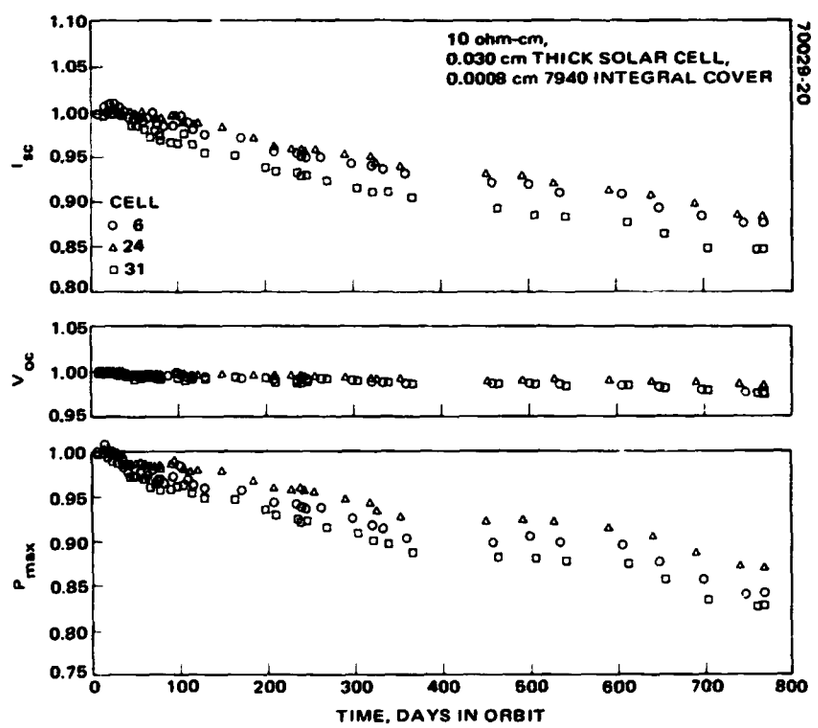

f) CONFIGURATION 6

FIGURE 11 (CONTINUED). IN-ORBIT NORMALIZED CELL PARAMETERS

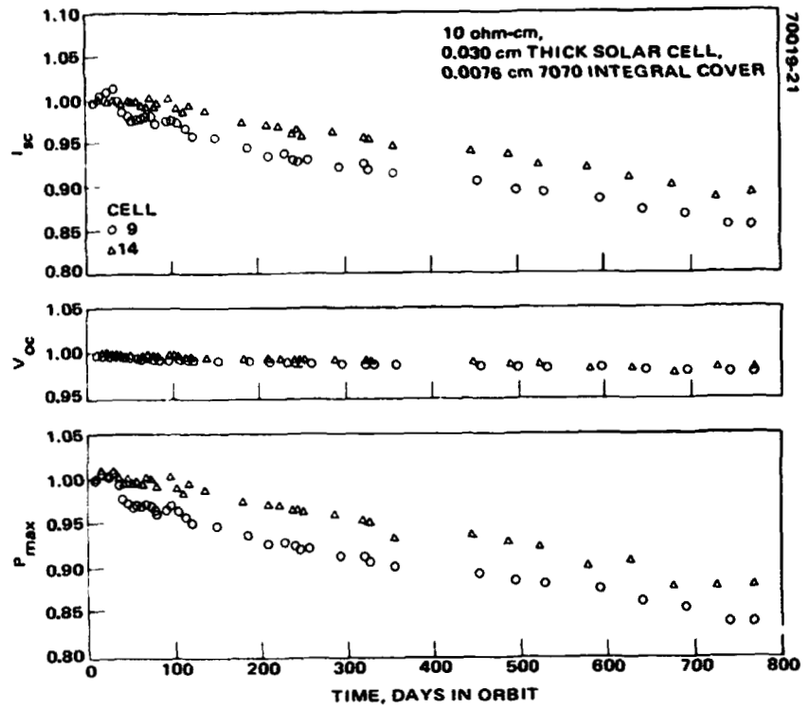

g) CONFIGURATION 7

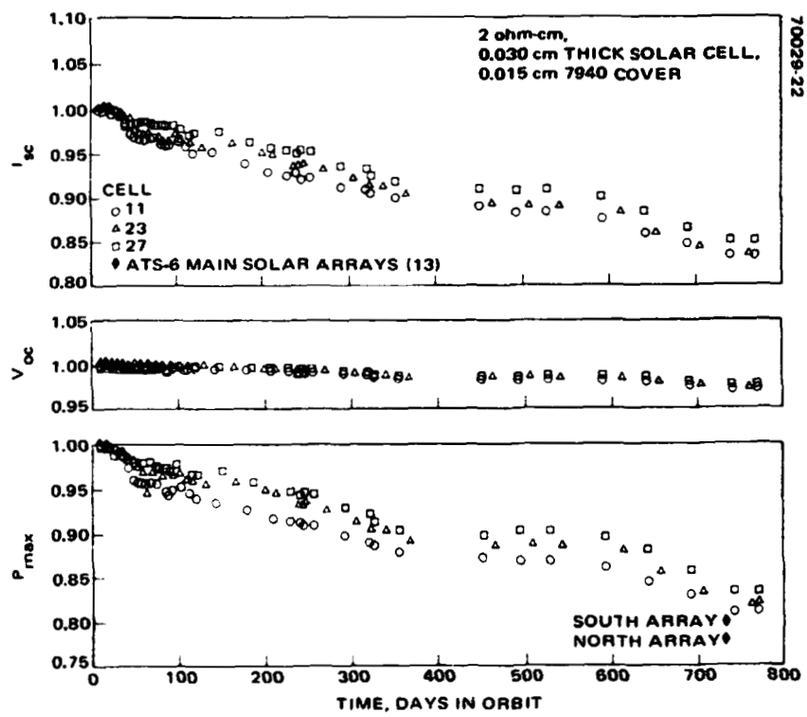

h) CONFIGURATION 8

FIGURE 11 (CONTINUED). IN-ORBIT NORMALIZED CELL PARAMETERS

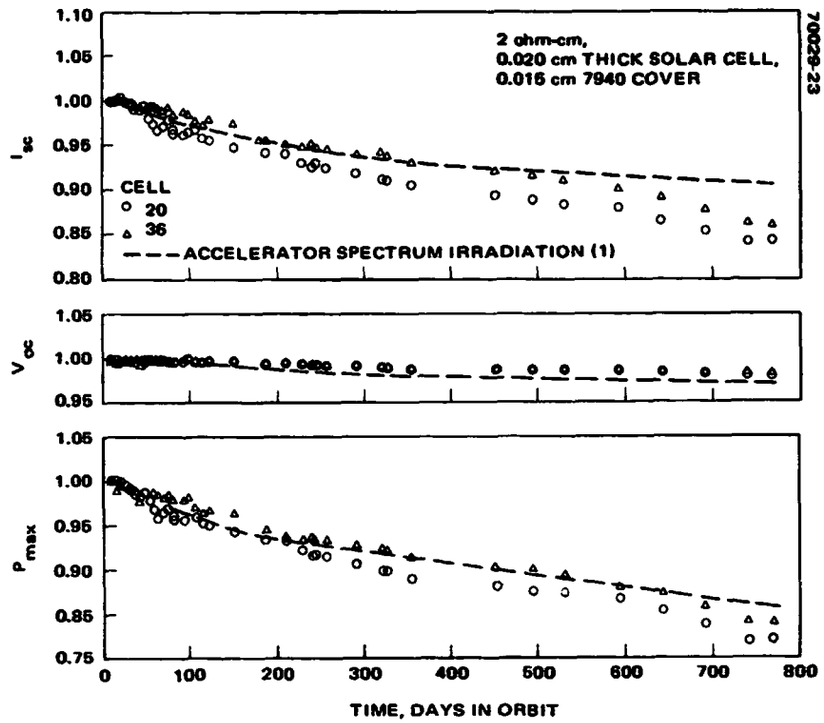

i) CONFIGURATION 9

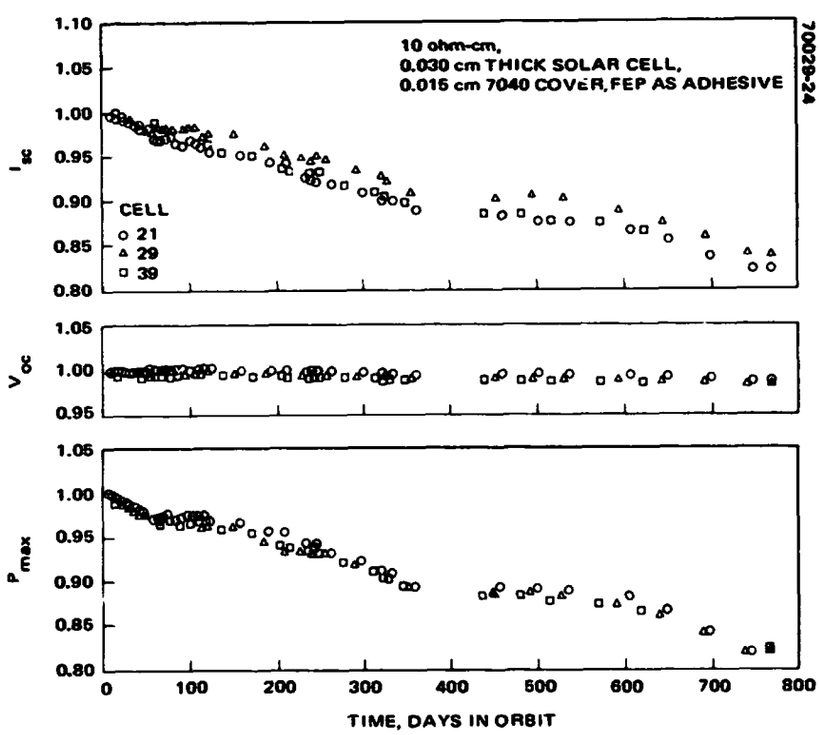

j) CONFIGURATION 10

FIGURE 11 (CONTINUED). IN-ORBIT NORMALIZED CELL PARAMETERS

cover; therefore, as little as 0.0038 cm (1-1/2 mils) covering will protect the cell from the low energy proton environment. This result is consistent with the results of the LES-6 experiment (Reference 11).

Profiles for configurations 8 and 9 display the normalized cell parameters for the 2 ohm-cm solar cells. In theory, the 2 ohm-cm cell performs higher than the 10 ohm-cm cell at beginning of life but degrades faster under the same particulate environment. The initial average cell maximum power for the 2 ohm-cm, 0.030 and 0.020 cm thick cells was 61.0 and 58.3 mW, respectively, and, for the 10 ohm-cm, 0.030 and 0.020 cm thick cells, 59.6 and 56.2 mW, respectively. After 2 years in synchronous orbit, the average cell maximum power for the 2 ohm-cm, 0.030 and 0.020 cm thick cells was 50.0 and 48.6 mW, respectively, and for the 10 ohm-cm, 0.030 and 0.020 cm thick cells, 49.2 and 48.0 mW, respectively. The 2 ohm-cm cells still have a slight advantage in power after 2 years in synchronous orbit. The average rate of degradation of the 2 ohm-cm cells compared to the 10 ohm-cm cell is slightly higher. The average percentage degradations to the cell parameters is shown in Table 5. Also shown in the configuration 8 profile is the 2 year power degradation for the ATS-6 main solar arrays. The ATS-6 main array consists of 2 x 4 cm, 0.034 cm (14 mil) thick, 2 ohm-cm solar cells with 6 mil, 0211 microsheet covers. The south solar array degraded about 20 percent and the north solar array degraded about 22 percent (Reference 13). Two differences in the cell/cover parameters might account for some additional degradation: 1) the cells were slightly thicker; 2) the covers were 0211 microsheet. Both conditions would cause slightly greater degradation to the ATS-6 main array than to the experiment cells. Cell thickness could account for 1 to 2 percent additional degradation and microsheet about 2 percent additional degradation. Taking these differences into account, the amounts of degradation to the ATS-6 main solar arrays and to the ATS-6 solar cell experiment configuration 8 appear to be very close. These degradation results, however, are not consistent with degradation observed for the Hughes Aircraft Company solar arrays in synchronous orbit.

One of the most interesting results of the ATS-6 experiment is shown in the profile for configuration 10, the solar cell coverglass configuration with FEP as an adhesive. The 7940 coverglass had an antireflecting coating but no UV filter. The degradation rates of this configuration are almost identical to those of configuration 2, its counterpart. There appears no more than the observed early 2 percent loss in I_{sc} due to UV effects, even though the FEP is unprotected from the UV environment. This combination of using FEP as a cover adhesive and a cover without an UV rejection filter could prove to be a very promising cost savings feature for solar array designs.

The cell degradation profiles for configuration 11 are those of the 0.020 cm thick 10 ohm-cm cell. Configuration 2 is the configuration's counterpart. As indicated in Table 3, the maximum power capability of this thinner cell is less than the 0.030 cm cell, 56.2 and 59.6 mW, respectively. The rate of degradation for the 0.020 cm cell is slightly less than

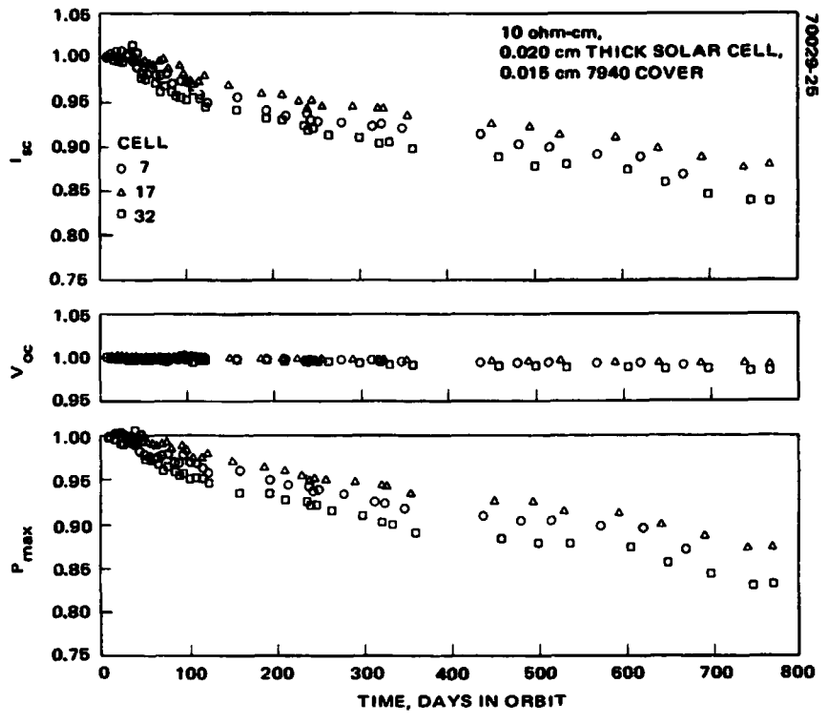

k) CONFIGURATION 11

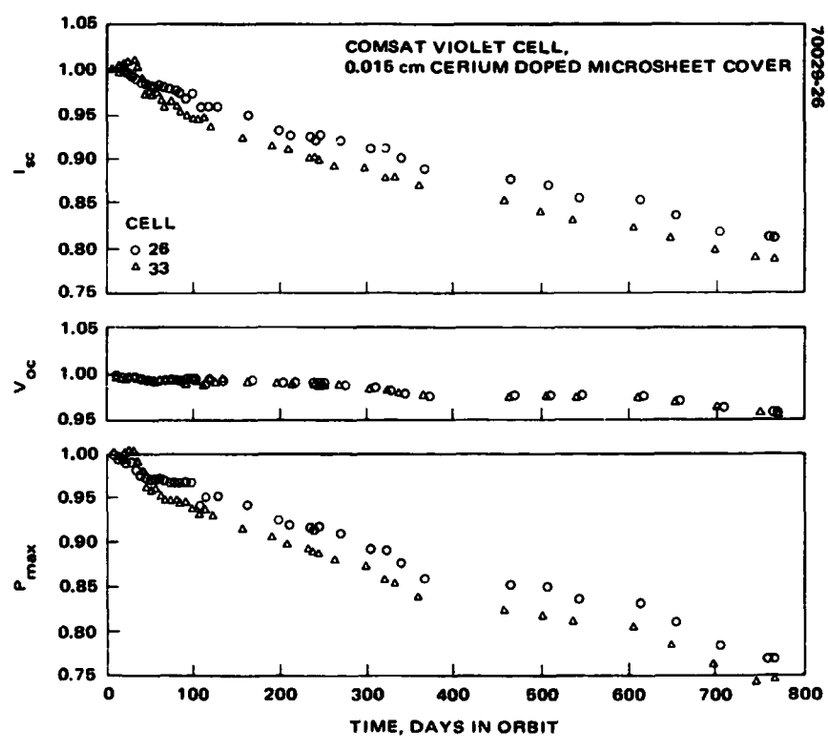

l) CONFIGURATION 12

FIGURE 11 (CONTINUED). IN-ORBIT NORMALIZED CELL PARAMETERS

that of the 0.030 cm cell, 14.7 and 17.4 percent, respectively. Again, the cells of configuration 11 display the same amount of individual cell dispersion in their degradation profiles as seen before.

The COMSAT violet cell degradation profiles are displayed in the figure for configuration 12. The violet cell not only had the highest beginning of life performance of all cell types, 82.5 ±1.1 mW, but the highest rate of degradation to all cell parameters, excluding the FEP covered cells (configuration 13). The average percentage degradation to I_{sc}, V_{oc}, and P_{mp} after 2 years in orbit was 19.4, 4.2, and 24.4 percent, respectively. From the published literature (Reference 14), the maximum power degradation to the violet cell is predicted to be 5 percent, much less degradation than observed. Nevertheless, the violet cells, after 2 years in orbit, are still outperforming all other cells with a maximum power capability of 62.4 ±1.0 mW.

Configuration 13 uses FEP as a cover material. These FEP-covered cells behaved very similarly to their counterpart, configuration 2, up to the first eclipse season. The eclipse seasons are indicated in the configuration 13 profile. As shown in this figure, the rate of degradation of V_{oc} and P_{mp} changes during the first eclipse season, indicating that the additional degradations to these cells is related to thermal stresses of the solar eclipses. Figure 12 displays the individual cell uncorrected current-voltage characteristics for cells 18 and 34 of configuration 13. Considerable softening of the I-V curve is indicated after 1 and 2 years. It appears shunting is occurring which would indicate low energy proton damage. Also, there appears that the series resistance has increased as indicated by the large degradations to the voltage parameter. Possible causes of the additional degradation are: 1) degradation of the FEP cover, e.g., from cracks, pinholes, or delaminations at the edges of the cell – this condition could result in low energy proton damage; 2) a thermal mismatch between the silicon, ohmic contact, interconnect, and FEP materials – this condition might result in the interconnect pulling away from the silicon, causing junction damage or an increase in series resistance. It should be noted that these FEP-covered cells represent 1972 technology.

Because of the high interest expressed in the advanced cell/cover parameters, the maximum power output through 2 years in synchronous orbit of six cells representing configurations 2, 5, 7, 8, 12, and 13 has been displayed in Figure 13.

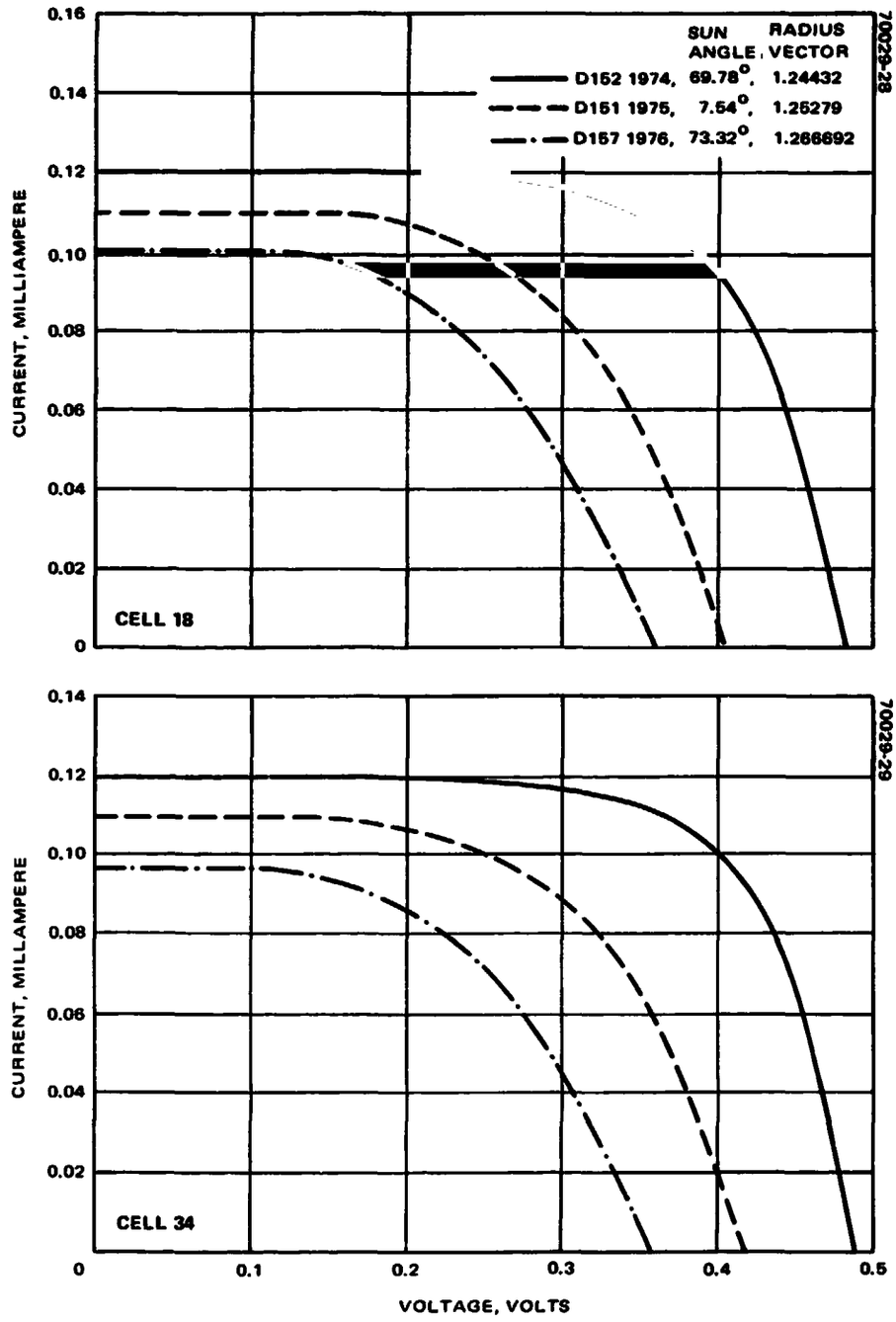

FIGURE 12. UNCORRECTED CURRENT VOLTAGE CHARACTERISTICS FOR CELLS OF CONFIGURATION 13

PRECEDING PAGE BLANK NOT FILMED.

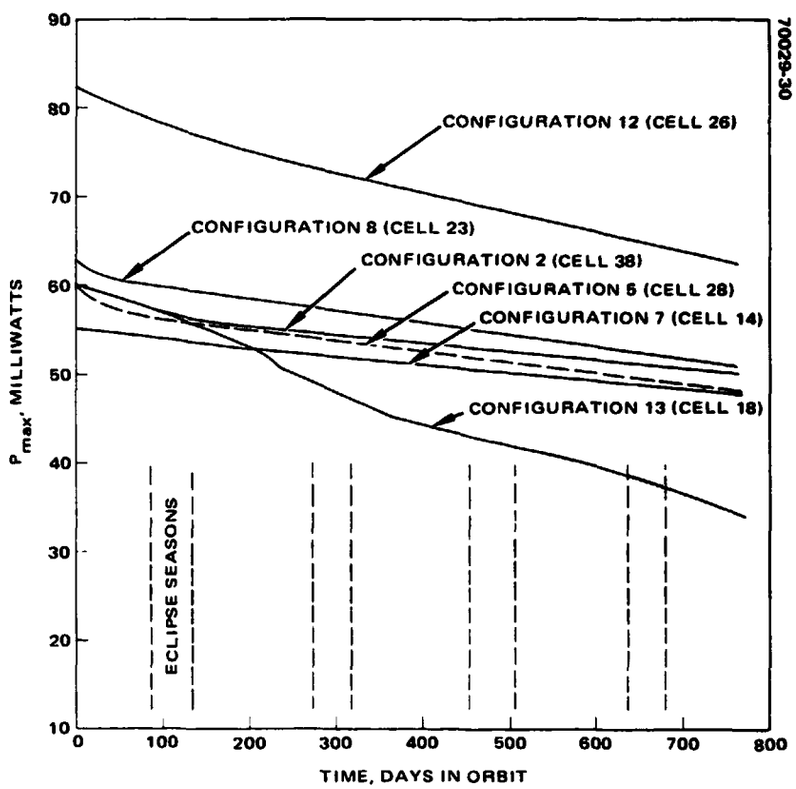

FIGURE 13. MAXIMUM POWER PERFORMANCE OF SIX CONFIGURATIONS THROUGH 2 YEARS IN ORBIT

6. CONCLUSIONS

1. The solar cell data indicated I_{sc} higher by 5 to 10 mA in space compared to measurements made with the pulsed xenon solar simulator. The higher I_{sc} performance in space is suspected to be due to an electronic offset rather than to any uncertainty in solar simulation.

2. The maximum power capability of the COMSAT violet cell was 35 percent greater than that of the 2 ohm-cm cell at beginning of life and still 25 percent higher after 2 years in orbit, even though degradation was more rapid.

3. For the conventional cells at beginning of life, the 2 ohm-cm, 0.030 cm thick cell performed 3.0 percent higher than the 10 ohm-cm cell of the same thickness; 4.6 percent greater than the 2 ohm-cm, 0.020 cm thick cell; and 8.3 percent greater than the 10 ohm-cm, 0.020 cm thick cell.

4. After 50 days in orbit (~400 sun hours), it appears that for conventionally covered cells the UV irradiation degrades current by approximately 2 percent. FEP used as an adhesive appears to be affected similarly even without the presence of an UV filter. Adhesive degradation without the protection of the UV filter appears to be about 3 percent after 50 days in orbit and an additional 3 percent after 2 years in orbit.

5. The FEP-covered cells (configuration 13) performed as well as their counterparts until the first eclipse season, where the rate of degradation increased. Forty-three percent power degradation has been experienced in 2 years of synchronous operation.

6. FEP as a cover adhesive with no UV protection performs as well as its counterpart.

7. After 2 years in orbit, the COMSAT violet cell has the highest performance (62 mW). This configuration also experienced the greatest rate of degradation (configuration 13, FEP-covered cell, excluded). The 2 ohm-cm conventional cells still exhibit a slight maximum power advantage over the 10 ohm-cm cells.

8. The current and power degradations after 2 years in orbit are greater than expected compared with laboratory electron spectrum irradiation and Hughes experience with solar arrays in orbit.

9. Degradation of cells with integral covers was among the lowest of all configurations. Hence, the need for thicker covers for radiation protection in synchronous orbit is questionable, at least during solar minimum.

10. In spite of the variation of cover thicknesses on the experiment, it was not possible to deduce a relationship between degradation and cover thickness. Increased protection with thick covers was not realized beyond the scatter of the data.

7. NEW TECHNOLOGY

This report does not contain items of new technology developed by Hughes Aircraft Company under this contract.

8. REFERENCES

1. L. J. Goldhammer and W. C. Dunkerly, Solar Cell Radiation Damage Experiment, Final Report, NASA Contract NAS 5-11677, 21 January 1974.

2. R. W. Opjorden, "Pulsed Xenon Solar Simulator System," Proceedings of the Eightn IEEE Photovoltaic Specialists Conference, August 1970.

3. L. J. Goldhammer and J. Patrick Corrigan, "Early Results of the ATS-6 Solar Cell Flight Experiment," Proceedings of the Eleventh IEEE Photovoltaic Specialists Conference, May 1975.

4. L. J. Goldhammer, "ATS-6 Solar Cell Flight Experiment after 325 Days in Synchronous Orbit," IEEE Transactions on Aerospace and Electronic Systems, Vol. AES-11, No. 6, November 1975.

5. L. J. Goldhammer, Solar Cell Radiation Damage Experiment, Addendum to Final Report (Angle of Incidence Test Report), NASA Contract NAS 5-11677, 12 March 1976.

6. L. J. Goldhammer, Improvement/ATS-6 Solar Cell Experiment, Temperature Coefficient and Implementation Report, NASA Contract NAS 5-22873, 19 August 1976.

7. W. D. Brown, et al., "Computer Simulation of Solar Array Performance," Proceedings of the Sixth IEEE Photovoltaic Specialists Conference, March 1967.

8. G. S. Goodelle, et al., "High Vacuum UV Tests of Improved Efficiency Solar Cells," Proceedings of the Eleventh IEEE Photovoltaic Specialists Conference, May 1975.

9. L. J. Goldhammer, "Irradiations of Solar Cell Candidates for the ATS-E Solar Cell Flight Experiment," Proceedings of the Ninth IEEE Photovoltaic Specialists Conference, May 1972.

10. J. I. Vette and A. B. Lucero, "Models of the Trapped Radiation Environment," NASA SP-3024, Vol. III, Electrons at Synchronous Altitudes, 1967.

PRECEDING PAGE BLANK NOT FILMED

11. F. W. Sarles, Jr., and Alan G. Stanely, "Observed Degradation of the LES-6 Synchronous Solar Cell Experiment," Proceedings of the Eighth IEEE Photovoltaic Specialists Conference, August 1970.

12. L. J. Goldhammer and S. W. Gelb, "Synchronous Orbit Performance of Hughes Aircraft Company Solar Arrays," Proceedings of the Eleventh IECEC Conference, September 1976.

13. T. A. LaVigna and F. L. Hornbuckle, "The ATS-6 Power System: Hardware Implementation and Orbital Performance," Proceedings of the Eleventh IECEC Conference, September 1976.

14. D. J. Curtin and R. W. Cool, "Qualification Testing of Laboratory Produced Violet Solar Cells," Proceedings of the Tenth IEEE Photovoltaic Specialists Conference, November 1973.